



Synthesis and characterization of Sn–Mo mixtures as negative electrode materials for Li-ion batteries

Y. Liang*, Z.G. Tian, H.J. Liu, R. Peng

College of Chemical Engineering and Food Science, Xiangfan University, Xiangfan 441003, PR China

ARTICLE INFO

Article history:

Received 11 February 2010
Received in revised form 8 May 2010
Accepted 20 May 2010
Available online 27 May 2010

Keywords:

Chemical precipitation
Characterization method
Sn–Mo
Li-ion batteries

ABSTRACT

Sn–Mo powder mixtures were prepared by chemical precipitation, followed by annealing at 700 °C in hydrogen atmosphere. The microstructure, morphology, and electrochemical performance of the powders were investigated by X-ray diffraction (XRD), scanning electron microscopy (SEM), energy dispersive X-ray spectroscopy (EDS), inductively coupled plasma mass spectroscopy (ICP) and electrochemical methods. The Sn–Mo mixture exhibited an initial discharge capacity of 491 mAh g⁻¹ with a better capacity retention displaying 277 mAh g⁻¹ after 20 cycles. This is due to the smaller particle size and a uniform distribution of the tin particles in the molybdenum matrix that effectively minimizes the effect of the large volume changes and also maintains the mechanic stability and structural integrity of the electrodes during cycling. Therefore, the electrode of the Sn–Mo mixture prepared by chemical precipitation exhibited better cycle life.

© 2010 Elsevier B.V. All rights reserved.

1. Introduction

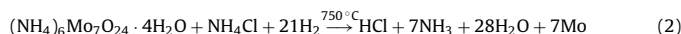
Tin-based compounds used as anode materials in lithium-ion batteries have attracted much attention in recent years [1–9]. It is due to displaying higher reversible specific capacities than carbon and the higher safety against the formation of lithium metal dendrites. Especially, tin-based metal alloys due to their low cost and high energy densities are the most exploited of alternative anode materials in lithium-ion batteries [10–19]. While tin metals can give high initial lithium insertion capacities, corresponding to a theoretical capacity of 990 mAh g⁻¹. On the other hand, volume changes by as much as 259% that occur during these alloying and dealloying reactions lead to mechanical disintegration of the anode resulting in cracking or pulverization of the electrodes [20]. In order to solve these problems, some inactive metals were introduced to improve the electrochemical properties. The active element is finely dispersed within an electrochemically inert matrix that acts as a buffer in order to maintain the mechanic stability and structural integrity of the electrodes during cycling. Moreover, the inactive matrix had better assure electronic and ionic conductivity throughout the electrode.

In order to fulfill these conditions, we have decided to use molybdenum as the inactive matrix since it is a fair electronic conductor and can improve the inter-particle connectivity [21]. However, it is difficult to obtain a highly-dispersed Sn–Mo

nanocomposite by mechanical milling process which always contains contaminations. The chemical precipitation technique has proved to be an economical way to produce homogeneous tin molybdenum nanoparticles, which provides a conventional procedure with the advantages of mild conditions, low cost, ease of work-up and promising large-scale production. Hence, in this paper, we intended to improve the initial coulombic efficiency of Sn by the addition of Mo, and for this purpose, Sn–Mo mixture was prepared by chemical precipitation.

2. Experimental

The precursor of Sn–Mo mixtures was prepared by a chemical precipitation method. Firstly, SnCl₄·5H₂O (0.02 mol) was dissolved in 200 ml distilled water. Secondly, ammonia aqueous solution was added drop by drop into the above solution until a pH value up to 10 under vigorous stirring. The white precipitates were subsequently obtained. Thirdly, (NH₄)₆Mo₇O₂₄·4H₂O was dissolved in 10 ml distilled water according to Sn:Mo = 1:0.5 (atomic ratio). The solution was added to the precipitates and magnetically stirred for 4 h before it was dried at 120 °C in the oven. Then the dried precursor was mixed uniformly. The Sn–Mo powders are produced by sintering the mixture at 750 °C for 2 h and then 700 °C for 6 h in hydrogen atmosphere. The reactions may be represented as follows (1) and (2):



The electrochemical performances of the above-mentioned Sn–Mo mixtures were tested. In a typical process, Sn–Mo powder mixtures were made into slurries containing 92 wt.% active materials, and 8 wt.% polyvinylidene di-fluoride (PVDF) in N-methyl pyrrolidinone (NMP), and were coated on copper foils. The coated electrodes were dried in a vacuum oven at 120 °C for 12 h. The electrodes were then pressed at the pressure of 2000 kg cm⁻². The cells were assembled in an argon filled glove-box (Mbraun, Unilab, Germany) using lithium metal foil as the counter elec-

* Corresponding author. Tel.: +86 710 359 3115; fax: +86 710 359 3115.
E-mail address: xfliangy@163.com (Y. Liang).

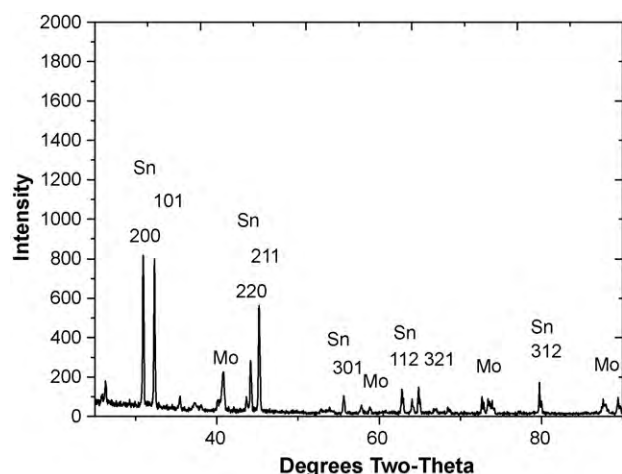


Fig. 1. XRD patterns of Sn–Mo mixture.

trode. The electrolyte was 1 M LiPF_6 in a mixture of ethylene carbonate (EC) and dimethyl carbonate (DMC) (1:1 by volume). The cells were galvanostatically charged and discharged under a constant current density of 0.15 mA cm^{-2} in the voltage range of 0.01–1.5 V. Charge–discharge tests were performed using a multi-channel battery cycling unit (Lisun, PCBT138-8D, China). The electrochemical properties of Sn–Mo as anodes in Li-ion batteries were tested via cyclic voltammetry (CV, CHI660, China). The CV and cycling testing were performed over the voltage range of 0.01–1.5 V versus a Li/Li^+ counter electrode.

The microstructure of mixtures was analyzed by X-ray diffraction (XRD, Y-2000) and scanning electron microscopy (SEM, JEOL 6700F). The chemical composition and impurities were determined with ICP emission spectroscopy (Perkin Elmer, Optima 2000DV) and energy dispersive X-ray spectroscopy (EDS, Oxford Instrument).

3. Results and discussion

Fig. 1 shows the X-ray diffraction patterns of the powder mixtures of a nominal composition of $\text{SnMo}_{0.5}$. All peaks in the scan range $20\text{--}90^\circ$ are attributed to the Sn and Mo phases. The diffraction peaks can be indexed to the three major peaks of Sn, namely, the (200), (101), and (211) diffractions were strong and clear, indicating the complete crystallization and corresponding well with standard ones of the cubic phase of tin. Meanwhile, the XRD peaks of Mo were weak and broad, displaying small crystallites (mostly amorphous) of Mo. The XRD patterns of the sample do not show any evidence for a new intermetallic phase or SnO_x , MoO_y .

ICP analysis shows that the exact composition of the sample is approximate $\text{Sn}_{0.65}\text{--Mo}_{0.35}$.

Fig. 2 presents the SEM image of Sn–Mo powders. The morphology of the microspheres with the particle size of about $0.2\text{--}2 \mu\text{m}$ was produced after the reduction of the $\text{Sn}(\text{OH})_4$ precursor. Meanwhile, the EDS analysis shows the spherical particles were elemental Sn. The fine Mo particles smaller than 100 nm were uniformly distributed on the tin surface or the interspaces between Sn spheres. This phenomenon is suspected to be due to melting Sn and a recrystallization and growth process associated to a high energy generated during reduction process. Moreover, the presence of Mo could separate metallic Sn and strongly decreased the size of Sn particles to a nano-scale. The free volume between the particles may accommodate volume changes during cycling.

Fig. 3 shows the variation of voltage versus charge–discharge (Li insertion) capacity for the Sn–Mo mixture. The sample exhibited an initial lithium storage capacity of 491 mAh g^{-1} and a stable reversible specific capacity of about 390 mAh g^{-1} . There is a plateau in the discharging curves around $0.01\text{--}0.4 \text{ V}$, which corresponds well with the formation of Li_xSn alloy. In the charging curves, there is a plateau around $0.5\text{--}0.85 \text{ V}$, which possibly is related to reform the Sn.

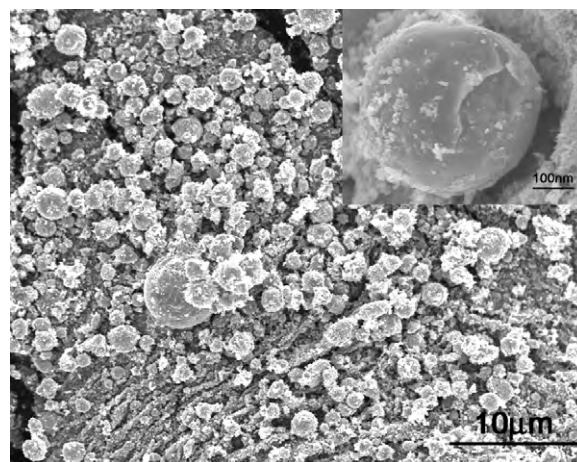


Fig. 2. SEM morphology of Sn–Mo mixture (the spherical particles were elemental Sn).

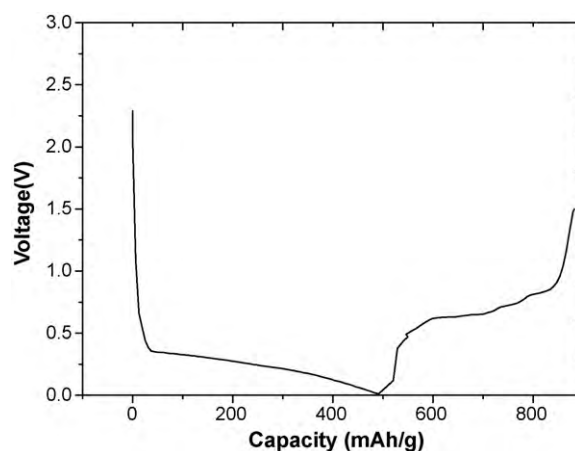


Fig. 3. The first discharge–charge curves of the Sn–Mo powders at a current density of 0.15 mA cm^{-2} .

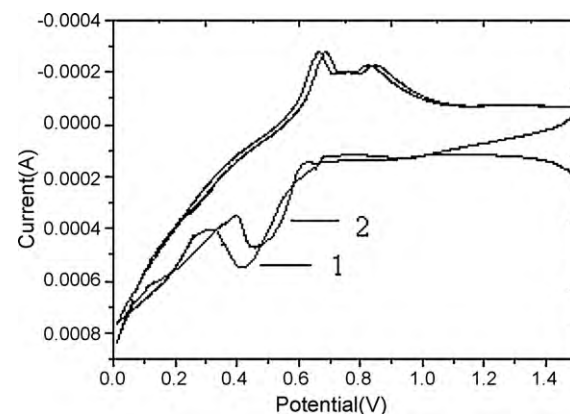


Fig. 4. The cyclic voltammetry curves of Sn–Mo electrodes.

The CV curves of Sn–Mo electrode (0.1 mV/s) are presented in Fig. 4. All cycles present the cathodic peak (about 0.4 V) and the anodic peak (about 0.65 V and 0.85 V), which are caused by reversible electrochemical oxidation and reduction of Sn with lithium [6,9,22,23]. The similarity suggests a common mechanism for the insertion and deinsertion of Li ions in all of these Sn-based electrodes.

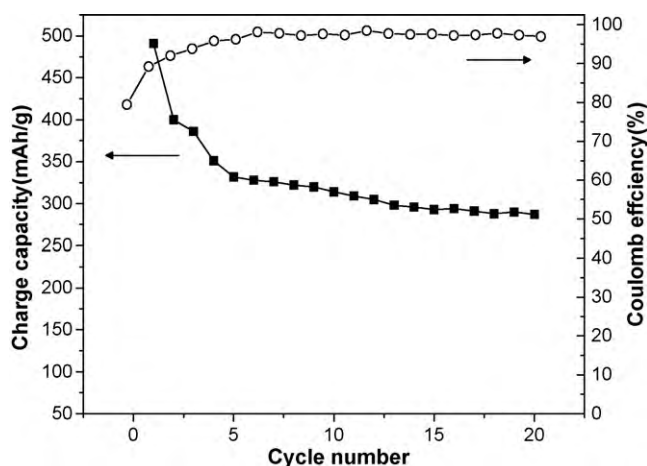


Fig. 5. Cycle performance of Sn–Mo electrodes.

The cycleability of Sn–Mo mixture is shown in Fig. 5. Thackeray et al. [22] and Kepler et al. [23] stated that the pure tin electrode provides a significantly higher capacity on the initial charge (670 mAh g^{-1}), but the capacity of the pure tin electrode decreases rapidly on cycling, dropping to $\sim 100 \text{ mAh g}^{-1}$ after 20 cycles. By contrast, the Sn–Mo mixture shows lower capacity (491 mAh g^{-1}), but improved stability to electrochemical cycling. It is suspected that addition of the Mo content improves retention capacity at the expense of reversible capacity because the transition element acts as an inert component in the electrochemical process.

The Sn–Mo electrodes have the highest coulomb efficiency (80%) in the first cycle and show little capacity fading over 20 cycles. The gravimetric first charge (Li extraction) capacity was 390 mAh g^{-1} , but the volumetric discharge capacity of more than 3100 mAh/cm^3 , which was translated using a density of Sn–0.5Mo, 8.14 g/cm^3 , was three times larger than that of graphite electrode. Meanwhile, the reversible capacity and retention rate of the materials synthesized by chemical precipitation process are superior to that of samples by mechanical milling method [24]. It may be suspected that the key to good cycleability is due to better contact between Sn and Mo particles and maintaining tin in high dispersion throughout charging and discharging. The homogeneous precursor of tin and molybdenum composites is beneficial to form highly-dispersed Sn–Mo mixtures and easily obtain the nano-scale particles.

The surface of every spherical tin is rough and the Mo particles tended to be around the Sn spheres, which facilitate the maintenance of the better structural integrity of the Sn–Mo mixtures and prevent the tin from particles to larger clusters. Meanwhile, spherical particles with the smaller specific surface areas and the larger contact areas between the nano-scale particles, which maximizing the rate capability benefits of shorter diffusion pathways and efficient intergrain electronic contacts, can increase the initial coulombic efficiency. Furthermore, the replacement of tin with molybdenum caused the structural disorder, which results partially in a suitable matrix to accommodate the volume change and dissipate local mechanical stresses. Therefore, based on the above results, it can be concluded that the Sn–Mo mixture synthesized by chemical precipitation followed by solid state reduction is promising for use as anodes for lithium-ion batteries.

4. Conclusion

Sn–Mo synthesized by chemical precipitation followed by solid state reduction was found to electrochemically insert and extract lithium without any conductive materials. The discharge capacity of the Sn–Mo mixture was estimated up to 491 mAh g^{-1} , and a reversible volumetric capacity of 3100 mAh/cm^3 , which is three times larger than that of graphite electrode. Furthermore, the cycling stability of Sn–Mo electrode was obviously improved for Sn–Mo mixture prepared by chemical precipitation followed by solid state reduction. Meanwhile, Sn–Mo electrode exhibited the highest coulomb efficiency (80%) in the first cycle and little capacity fading over 20 cycles. It was considered that the fine Mo particles were uniformly distributed on the spherical tin surface provided a better contact area and enhanced the interface strength between the active materials, and thus, the cycle performance was improved.

Acknowledgements

This work was supported by the Natural Science Funds of Hubei Province (No. 2009CDZ037) and the major projects funding of Hubei Province Department of Education (No. Z20102601).

References

- [1] F. Belliard, J.T.S. Irvine, *J. Power Sources* 97–98 (2001) 219–222.
- [2] N. Pereira, L.C. Klein, G.G. Amatucci, *Solid State Ionics* 167 (2004) 29–40.
- [3] R. Zhang, J.Y. Lee, Z.L. Liu, *J. Power Sources* 112 (2002) 596–605.
- [4] J.H. Harreld, J. Sakamoto, B. Dunn, *J. Power Sources* 115 (2003) 19–26.
- [5] Y. Wang, J.Y. Lee, H.C. Zeng, *Chem. Mater.* 17 (2005) 3899–3903.
- [6] I.A. Courtney, J.R. Dahn, *J. Electrochem. Soc.* 144 (1997) 2943–2946.
- [7] Y. Liang, J. Fan, X.H. Xia, Y.S. Luo, Z.J. Jia, *Electrochim. Acta* 52 (2007) 5891–5895.
- [8] J.Y. Kim, D.E. King, P.N. Kumta, G.E. Blomgren, *J. Electrochem. Soc.* 147 (2000) 4411–4420.
- [9] I.A. Courtney, J.R. Dahn, *J. Electrochem. Soc.* 144 (1997) 2045–2052.
- [10] J.J. Zhang, X. Zhang, Y.Y. Xia, *J. Electrochem. Soc.* 154 (2007) A7–A13.
- [11] J.R. Dahn, R.E. Mar, M.D. Fleischauer, M.N. Obrovac, *J. Electrochem. Soc.* 153 (2006) A1211–A1220.
- [12] A.D.W. Todd, R.E. Mar, J.R. Dahn, *J. Electrochem. Soc.* 153 (2006) A1998–A2005.
- [13] N. Tamura, R. Ohshita, M. Fujimoto, S. Fujitani, M. Kamino, et al., *J. Power Sources* 107 (2002) 48–55.
- [14] H. Sakaguchi, H. Honda, Y. Akasaka, T. Esaka, *J. Power Sources* 119–121 (2003) 50–55.
- [15] Y.L. Kim, S.J. Lee, H.K. Baik, S.M. Lee, *J. Power Sources* 119–121 (2003) 106–109.
- [16] C. Arbizzani, S. Beninati, M. Lazzari, M. Mastragostino, *J. Power Sources* 158 (2006) 635–640.
- [17] E. Rönnebro, J. Yin, A. Kitano, M. Wada, T. Sakai, *Solid State Ionics* 176 (2005) 2749–2757.
- [18] H. Mukaibo, T. Sumi, T. Yokoshima, T. Momma, T. Osaka, *Electrochem. Solid State Lett.* 6 (2003) A218–A220.
- [19] N. Tamura, M. Fujimoto, M. Kamino, S. Fujitani, *Electrochim. Acta* 49 (2004) 1949–1956.
- [20] A. Sivashanmugam, T. Premkumar, S. Gopukumar, N.G. Renganathan, M. Wohlfahrt-Mehrens, J. Garche, *J. Appl. Electrochem.* 35 (2005) 1045–1050.
- [21] A. Fernández, F. Martín, J. Morales, J.R. Ramos-Barrado, L. Sánchez, *Electrochim. Acta* 51 (2006) 3391–3398.
- [22] M.M. Thackeray, C.S. Johnson, A.J. Kahaian, K.D. Kepler, J.T. Vaughey, et al., *J. Power Sources* 81–82 (1999) 60–66.
- [23] K.D. Kepler, J.T. Vaughey, M.M. Thackeray, *J. Power Sources* 81–82 (1999) 383–387.
- [24] Y. Liang, *J. Alloys Compd.* 474 (2009) 590–594.